

MATERIAL CHARACTERIZATION OF CANDIDATE SILICON BASED CERAMICS FOR STATIONARY GAS TURBINE APPLICATIONS

Vijay M. Parthasarathy, Jeffrey R. Price, William D. Brentnall
Solar Turbines Incorporated
San Diego, California

George Graves, Steven Goodrich
University of Dayton Research Institute
Dayton, Ohio

ABSTRACT

The Ceramic Stationary Gas Turbine (CSGT) Program is evaluating the potential of using monolithic and composite ceramics in the hot section of industrial gas turbines. Solar Turbine's Centaur 50 engine is being used as the test bed for ceramic components. The first stage blade, first stage nozzle and the combustor have been selected to develop designs with retrofit potential, which will result in improved performance and lowered emissions. As part of this DOE sponsored initiative a design and life prediction database under relevant conditions is being generated. This paper covers experiments conducted to date on the evaluation of monolithic silicon based ceramics. Mechanical property characterizations have included dynamic fatigue testing of tensile as well as flexural specimens at the temperatures representative of the blade root, the blade airfoil and the nozzle airfoil. Data from subcomponent testing of blade attachment concepts are also included.

INTRODUCTION

Silicon based ceramics have been evaluated for heat engine applications since the 1970s. The principal thrust of these efforts have been directed towards automotive engines as well as rocket and missile engines. Since these applications do not typically require lives in excess of 5000 hours, a long term database for the candidate ceramics has not been adequately developed. Industrial gas turbines, on the other hand typically require tens of thousands of hours of operation between overhaul. Therefore a critical part of the CSGT program has been the establishment of a long term database under relevant engine conditions. Table 1 lists the candidate ceramics for the hot section of the Centaur 50 gas turbine. Primary metallic components selected for replacement with ceramic materials are the first stage blade, the first stage nozzle and the combustor liners. The testing strategies for the blade, the nozzle and the combustor are given below:

Blade

For the ceramic insertion version of the Centaur 50 engine the

TABLE 1. CANDIDATE MONOLITHIC CERAMICS

Name	Component
NAC's NT-164 Hipped Silicon Nitride	Blades
NAC's NT-164 Hipped Silicon Nitride	Nozzles
NAC's NT-230 Reaction Bonded Silicon Carbide	Combustor Rings
CC's GN-10 HIPed Silicon Nitride	Blades
Kyocera's SN-253 Gas Pressure Sintered Si_3N_4	Blades
NGK'S SN-88 Gas Pressure Sintered Si_3N_4	Nozzles
Carborundum's Hexoloy SA Alpha Sintered Silicon Carbide	Nozzles
Carborundum's Hexoloy SA Alpha Sintered Silicon Carbide	Combustor Tiles
B.F. Goodrich's SiC/SiC	Combustor Liner
Babcock and Wilcox's Al_2O_3/Al_2O_3	Combustor Liner
Dupont Composite's SiC/SiC	Combustor Liner

design operating temperatures of the blade airfoil and the blade root are below 1093 °C (2000° F). The failure modes of principal concern for this component are fast fracture and slow crack growth. The following tests were planned for the blade candidate materials:

- 1) Dynamic fatigue testing (2 decades difference in crosshead speed) of machined flexure bars at 760°C (1400°F).
- 2) Dynamic fatigue testing (2 decades difference in crosshead speed) of as-fired flexure bars at 1093°C (2000°F), simulating the airfoil.
- 3) Fast fracture testing at relevant temperatures, to complete the database.
- 4) Static flexure fatigue testing at 760°C (1400°F) for up to 4000 hours.

Compliant Layer and Subcomponent Testing Blade attachment testing involves the evaluation of various ceramic blade root configurations under static and cyclic loading. Because ceramic blade to metallic disk attachments typically degrade due to the combination of centrifugal (CF) blade loads on a ceramic to metallic interface and relative motion (tangential sliding) at the loaded interface due to differential thermal expansion of the ceramic blade and metallic disk, the CSGT attachment testing focuses on these two primary conditions.

Nozzle

Failure modes for the nozzle could be fast fracture, slow crack growth or creep because the peak temperature could be as high as 1288°C (2350°F). Also the peak stress location coincides with the maximum temperature. Therefore the test plan includes investigation of all three potentially life limiting modes. Oxidation is a subset of the long term stress tests but will also be evaluated for its effect on fast fracture.

- 1) As-fired flexure bar testing at two different crosshead speeds (2 decades different). Test temperature of 1288°C (2350°F).
- 2) Dynamic fatigue testing in tension at two different crosshead speeds (4 decades different).
- 3) Tensile stress relaxation tests at 1300°C (2372°F).
- 4) Tensile stress rupture testing of tensile rods for up to 10,000 hours.

Combustor

The peak temperature of the combustor rings and tiles is in the 1150-1205°C (2100-2200°F) range. Since it has been established that silicon carbides show very little time dependent degradation at this temperature, the primary failure mode of concern is fast fracture. This information is available in literature. Sticking due to formation of glassy surface layer between adjacent tiles and rings is possible and tests to evaluate this problem are underway.

EXPERIMENTAL PROCEDURE

The previously described tests are being carried out at three locations, Solar, University of Dayton Research Institute (UDRI) and Oak Ridge National Laboratory (ORNL). As part of the effort, 25 tensile creep frames were purchased from Advanced Test Systems

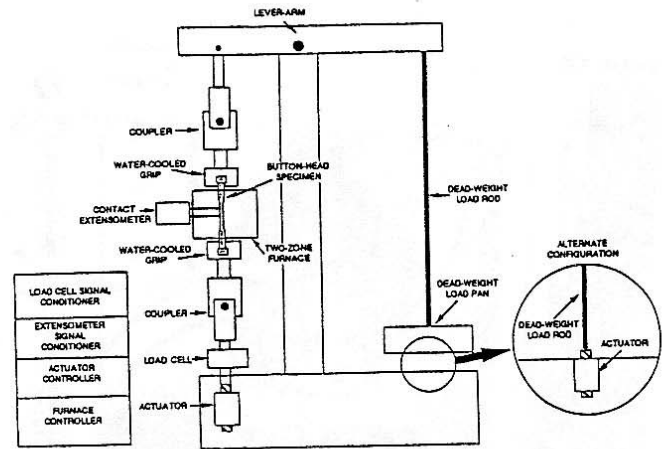


FIGURE 1. SCHEMATIC REPRESENTATION OF THE STRESS RUPTURE MACHINE AT ORNL

(ATS). The test facilities and the experimental procedure at each of the facilities is given below.

Figure 1 is a schematic representation of the creep/stress rupture test machine that will be used by ORNL. The test frames at Solar and UDRI are very similar to this machine. The primary differences are that ORNL uses a contact extensometer, Solar uses laser extensometers and UDRI uses a customized laser speckle interferometer system to measure strain. Solar also uses an MTS hydraulic system for flexural and cyclic fatigue testing.

Sintered silicon nitride and silicon carbide specimens were used in this study. The tensile specimens are cylindrical in shape with buttonheads for gripping and a smooth transition to the tensile gage section. The buttonhead tensile specimens having a nominal gage length of 35 mm (1.38 in.) and a diameter of 6.35 mm (.25 in.) are used. The final grinding direction in the gage and transition section is normally longitudinal, to minimize the stress concentrations at artificially induced surface flaws.

The flexure specimens were supplied both in the machined and the as-fired condition. Typically the machining direction is parallel to the longest side of the bar, but some samples have been deliberately machined with the direction at 90° to the specimen long axis. These specimens are used to evaluate the effects of different machining parameters. The dimensions of the flexure bars were 3 x 4 x 45 mm (MIL-STD-1942(A) specimen size B) with the outer span being 40 mm (1.57 in.) and the inner span being 20 mm (0.78 in.). The machined flexure bars were ground to a 0.4 micrometer (16 microinch) finish. The as-fired surface acted as the tensile face in the tests.

Flexural strength was measured in four point bending following MIL-STD-1942. The tests specimens were loaded at crosshead speed rates of 0.004 cm/s (0.095 in./min.) and 0.00004 cm/s (0.00095 in./min). Elevated temperature flexural tests were conducted in high temperature furnaces attached to the test machine.

Stress rupture tests (static fatigue) are being conducted by first heating the tensile specimen in a high temperature furnace to 1288°C (2350°F) and then applying the required load on the specimen. The weights. The stress rupture machines at UDRI and ORNL have the ATS stress rupture machines have a 20:1 lever arm and use free added

feature of being able to load the unfailed specimens to failure in fast fracture mode.

Fracture origins were identified and characterized by light microscopy and scanning electron microscopy (SEM). The microstructure of the candidate materials were also studied using light microscopy and SEM on polished and etched specimens and on fractured surfaces. Energy Dispersive X-ray analysis was used for composition determination.

Dovetail root and pinned root attachment specimens were supplied by AlliedSignal Ceramic Components (GN-10), Kyocera Industrial Ceramics Corporation (SN-253) and Norton Advanced Ceramics (NT-164) for testing in an Instron tensile testing apparatus. The grips for the attachment specimen testing were constructed from Waspalloy, which is the disk material that will be used for actual engine testing. Figure 2 shows a pinned root attachment specimen test in progress. The attachment testing is being conducted at loads representing full CF load conditions, cyclic temperature and CF load conditions, and room and elevated temperature failure loads. The behavior of various compliant layer configurations for the dovetail blade attachment specimens at these conditions is also being evaluated. Prior to each test, the specimens are inspected dimensionally and visually at 40X magnification. Following each test the specimens are carefully examined both visually and microscopically to determine the failure origin and mechanism for failure.

RESULTS AND DISCUSSION

Dynamic Fatigue Testing for Blades

Dynamic Fatigue Testing at Room Temperature. Room temperature strength degradation of silicon nitrides has been reported in the literature (Hecht et al, 1990). The available database was reviewed for the three candidate materials NT 164, GN-10 and SN 253. Dynamic fatigue strength data as a function of crosshead speed was found in the literature for NT 164 and SN 253 (Carruthers et al., 1994). Solar conducted dynamic fatigue strength tests for GN-10 on machined flexure bars. Table 2 gives the results of this test. The mean strength showed a deterioration from 796 MPa (115.46 Ksi) to 659 MPa (95.58 Ksi) at the lower crosshead speed. The slow crack growth exponent of approximately 24, is the lowest among the candidate materials. (The lower the exponent, the greater is the tendency of this material to exhibit slow crack growth.)

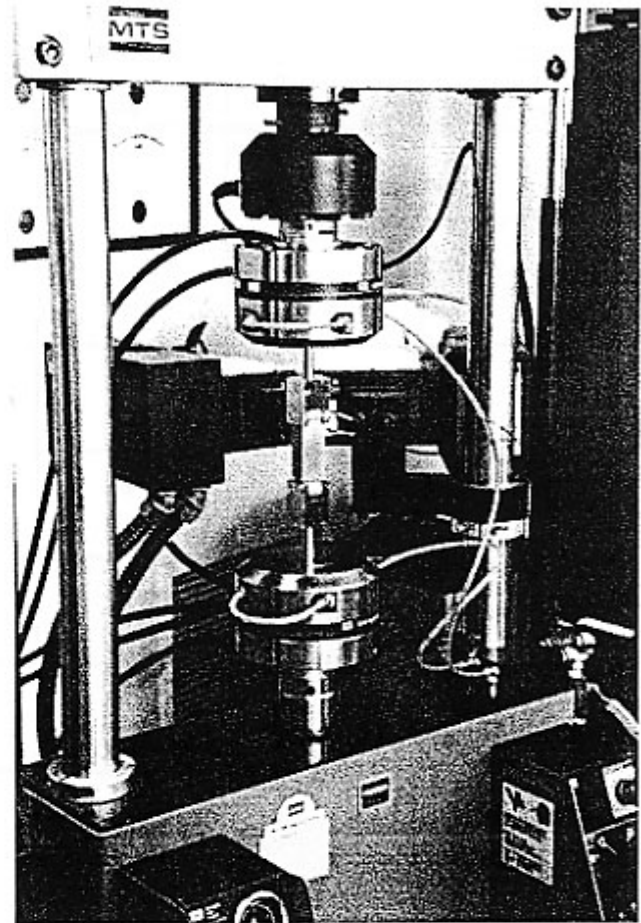


FIGURE 2. PINNED ROOT ATTACHMENT TEST IN PROGRESS

The slow crack growth exponent for the other two materials NT 164 and SN 253 were determined as 26 (not significantly different from GN10) and 100 respectively. Since SN253 does not have machined surface remnants of HIP encapsulants that can weaken the parent material, it exhibits better strength retention.

TABLE 2. ROOM TEMPERATURE DYNAMIC FATIGUE TESTING RESULTS

Mat/Prop	Number of Specimens Tested	Avg Strength Mpa (Ksi)	Weibull Modulus m	Standard Deviation Mpa (Ksi)	Slow Crack Growth Exponent (n)
GN-10 0.004 cm/s (0.095 in/min)	10	796 (115.46)	10	81 (11.8)	24
GN-10 0.00004 cm/s (0.00095 in/min)	10	659 (95.58)	9	78 (11.28)	

TABLE 3. DYNAMIC FATIGUE TESTING AT 760°C (1400°F)

Matl/Prop	Number of Specimens Tested	Avg Strength Mpa (ksi)	Weibull Modulus m	Standard Deviation Mpa (ksi)	Slow Crack Growth Exponent (n)
SN 253 0.004 cm/s (0.095 in/min)	20	790 (114.6)	10	82 (11.96)	112
SN 253 0.00004 cm/s (0.00095 in/min)	20	758 (109.9)	13	59 (8.62)	
NT 164 0.004 cm/s (0.095 in/min)	20	900 (130.6)	10	92 (13.3)	38
NT 164 0.00004 cm/s (0.00095 in/min)	20	800 (116)	9	83 (12.1)	
GN-10 0.004 cm/s (0.095 in/min)	20	674 (97.8)	14	43 (6.3)	28
GN-10 0.00004 cm/s (0.00095 in/min)	20	575 (83.4)	15	42 (6.1)	

25 microns

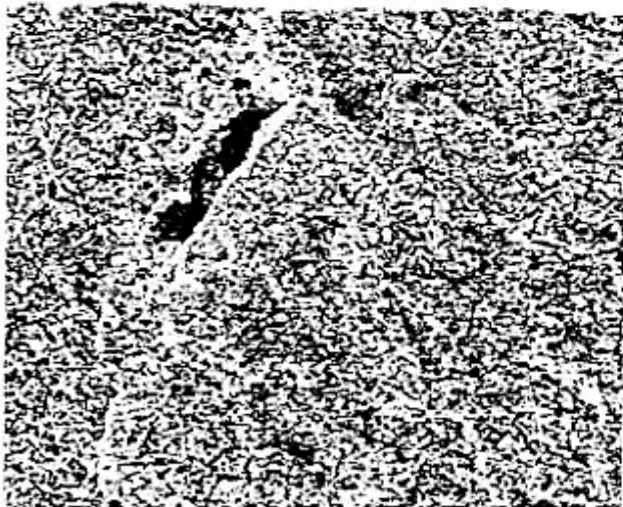


FIGURE 3. SCANNING ELECTRON MICROGRAPH OF FRACTURE INITIATION SITE- NT 164 (MAG 1000X)

One of the NT 164 flexure specimens fractured at an unusually low stress of 565 MPa (82 ksi) at the faster crosshead speed. A microstructural analysis of the specimen (Figure 3) indicated the



FIGURE 4. GLASSY POOLS ON NT 164 MACHINED SURFACE

source of failure to be a 38 micrometer (0.0015 inch) inclusion just below the surface. EDX analysis of the defect shows iron present in the inclusion. The presence of glassy pools with dendrites on the surface is the other major type of defect noticed (Figure 4). The SN253

of failure. It was more difficult to identify the starting point of failure for this material. The major feature of this material, noticed under the scanning electron microscope was the presence of small protrusions distributed evenly on the surface (Figure 5). A clear correlation between the origin of failure and these protrusions was not established.

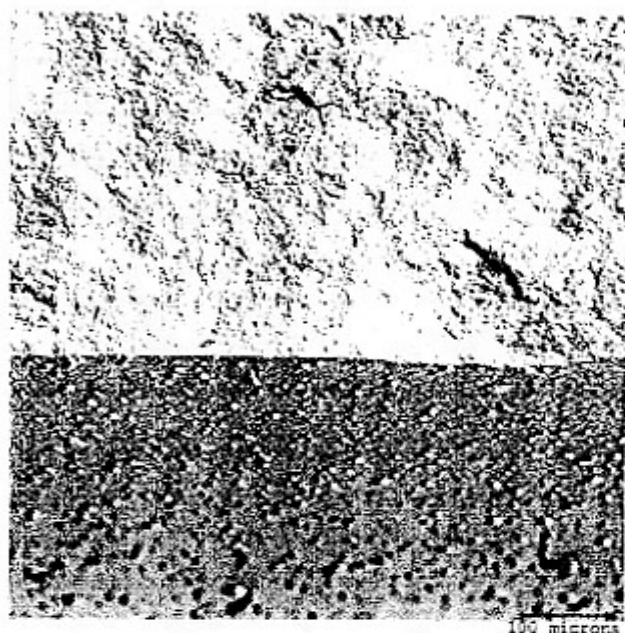


FIGURE 5. SN 253 SURFACE SHOWING REGULAR PROTRUSIONS. (MAG 1000X)

Dynamic Fatigue Testing at 1093° C (2000° F)

Since the airfoil of the blade can see a peak temperature of 1093° C (2000° F) and the ceramic airfoil is in the as-fired condition, as-fired flexure bars of one of the candidate materials, NT 164, were tested in dynamic fatigue at 1093° C (2000° F). Table 4 gives the results of this testing.

The strength degrades at a similar rate in going from the 0.004 cm/s (0.095 in/min) to 0.00004 cm/s (0.00095 in/min) crosshead speed as compared to the 760° C (1400° F) degradation for the machined NT 164 flexure bars. However, a negative feature of the as-

fired surface is the greater variability in going from specimen to specimen as compared to the machined surface. Failures originated at iron inclusions as well as pores on the surface.

Failure times were estimated using equations [1] and [2] (listed below) and the machined flexure data at 760° C (1400° F).

$$(\sigma_f/\sigma_{99})^n = tf/1 \text{ seconds} \quad (\text{Wiederhorn, et. al., 1974}) \quad [1]$$

where σ_f is the 99.0 % POS fast fracture strength,
 σ_{99} is the peak design stress,
 n is the slow crack growth exponent,
 tf is the time to failure in seconds, and assuming it takes 1 second at stress for a material to fail in fast fracture

$$\ln \ln (1/P_{11}) - \ln \ln (1/P_{12}) = m (\ln \sigma_1 - \ln \sigma_2) \quad [2]$$

Used to determine the 99% P.O.S. fast fracture strength in equation [1]

where P_{11} is the Probability of Survival under condition 1
 P_{12} is the Probability of Survival under condition 2
 σ_1 is the stress corresponding to condition 1
 σ_2 is the stress corresponding to condition 2
 m is the Weibull modulus

Calculations indicated that the time to failure is well in excess of 10,000 hours for the SN 253 as well as the NT 164 material, assuming the design stress for the flexure bar is 255 MPa (37 ksi).

Static Fatigue Testing For Blades

A 4000 hour static fatigue test on machined flexure bars is currently underway at ORNL. Test conditions are 260 MPa (37 ksi) at 760° C (1400° F). The test bars have accumulated 2500 hours of operation with two unplanned shutdowns. All three flexure bars have been inspected prior to testing using laser scattering. One of the flexure bars being tested has a pronounced iron defect on the surface.

Attachment Test For Blades

Table 5 summarizes the results of attachment testing for the dovetail root design to-date. At room temperature the dovetail specimens failed at stresses 3-4 times the nominal design stress. Figure 6 shows the failure origin of a failed dovetail attachment

TABLE 4. DYNAMIC FATIGUE TESTING OF AS-FIRED FLEXURE BARS AT 1093° C (2000° F)

Mat/Prop	No. of Specimens Tested	Avg Strength Mpa (ksi)	Weibull Modulus m	Standard Deviation Mpa (ksi)	Slow Crack Growth Exponent (n)
NT 164 0.004 cm/s (0.095 in/min)	10	634 (92)	7	101 (14.7)	44
NT 164 0.00004 cm/s (0.00095 in/min)	10	574 83.2	9	78 (11.3)	

TABLE 5. RESULTS OF DOVETAIL ROOT ATTACHMENT TESTING

Material	Test Temperature	Failure Stress*	Comments
GN-10 Si ₃ N ₄	Room Temperature	221 MPa (32 ksi)	Test performed in duplicate stopped at 100% design load.
GN-10 Si ₃ N ₄	Room Temperature	924 MPa (134 ksi)	Failure in dovetail neck section
NT164 Si ₃ N ₄	Room Temperature	855 MPa (124 ksi)	Failure in dovetail neck section
SN-253 Si ₃ N ₄	Room Temperature	745 MPa (108 ksi)	Failure in dovetail neck section
SN-253 Si ₃ N ₄	760° C (1400° F)	427 MPa (62 ksi)	Failure in dovetail neck section

* Average stress determined for the minimum cross section.

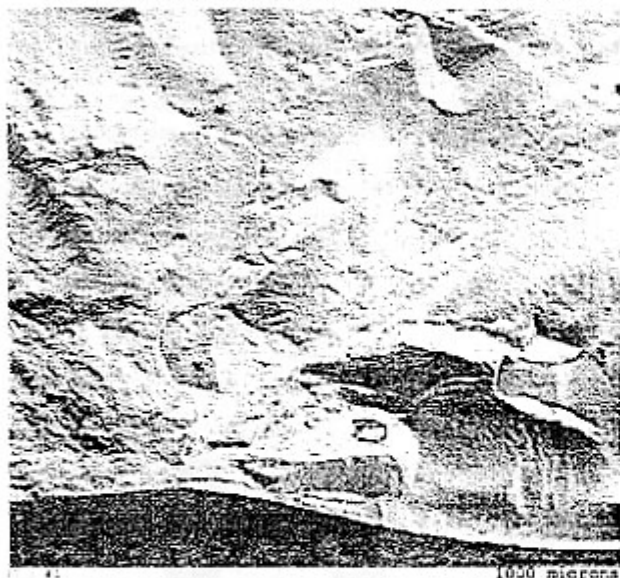


FIGURE 6. FAILURE ORIGIN OF DOVETAIL ATTACHMENT SPECIMEN

specimen. A thin (0.13 mm/0.005 in.) nickel compliant layer material was used for room temperature testing in order to simulate the behavior of the actual compliant layer material (nickel based alloy) at the elevated blade root temperature in actual service. The nickel compliant layer provided any deformations during loading which would identify uneven loading of the specimen during testing. The nickel based alloy is used for testing at 760° C (1400° F) which is the approximate steady state temperature of the blade root in service. Testing to date has shown that the selected compliant layer material has performed well under the blade root conditions.

A single test was performed at the steady state blade root temperature. The failure load in this test was markedly lower than in the room temperature test, but was over 2 times the design stress at actual engine operating conditions. Some locking up of the blade attachment specimen and compliant layer material in the metallic grip was observed in the test. This was partly due to opening of the dovetail grip (-0.006 in.) at the high load and elevated temperature. Minor evidence of contact stress was seen in the failed specimen and compliant layer material.

This spreading of the metallic grip should not occur in actual service since the disk attachment represents a stiffer structure and adjoining blades in the disk will counteract the opening of the dovetail attachment. Also the loads in the disk during actual service will be much lower than in these proof tests. Analysis of this test is continuing. Modification of the compliant layers is currently being evaluated in an attempt to minimize wedging, to provide more compliance at initial engine start-up, and to provide a measure of damping of the ceramic blade.

The results of the pinned root attachment specimens is given in Table 6. The pinned root attachment specimens failed at stresses between 540 and 620 MPa (78 and 90 ksi), which is close to the steady state stress level predicted for the design of this pinned root design. To evaluate the effect of surface finish, various combinations of attachment specimens and pins with different surface finishes (between r.m.s 8 and 30 microinch) were evaluated. Pins with a surface finish of r.m.s. 32 microinch exhibited failure at a radial machining mark (see Figure 7). Using pins with a surface finish of r.m.s. 8 microinch resulted in failure in the attachment root.

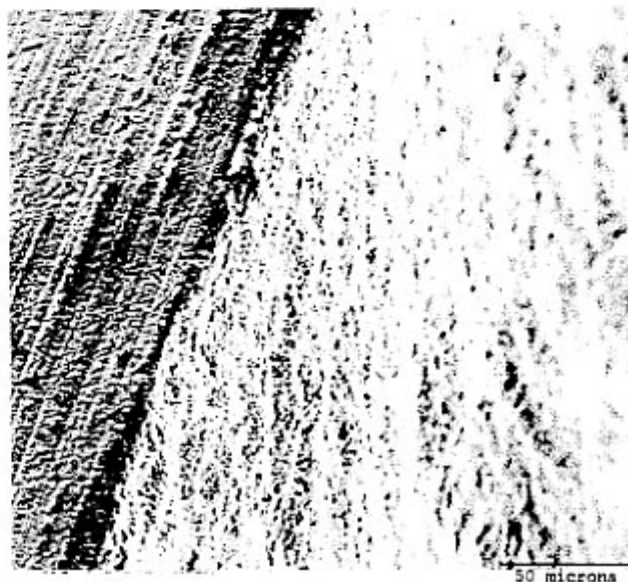


FIGURE 7. FAILURE ORIGIN OF PIN IN MACHINING GROOVE

TABLE 6. RESULTS OF PINNED ROOT ATTACHMENT TESTING

Attachment Specimen Material	Pin Material	Test Temperature	Failure Stress	Comments
GN-10 Si ₃ N ₄	GN-10 Si ₃ N ₄	Room Temperature	550 MPa (80 ksi)	Pin failure, internally initiated
GN-10 Si ₃ N ₄	SN-253 Si ₃ N ₄	Room Temperature	587 MPa (85 ksi)	Fracture in attachment
NT164 Si ₃ N ₄	NT164 Si ₃ N ₄	Room Temperature	540 MPa (78 ksi)	Pin failure in radial machining groove
SN-253 Si ₃ N ₄	SN-253 Si ₃ N ₄	Room Temperature	620 MPa (90 ksi)	Fracture in attachment
SN-253 Si ₃ N ₄	SN-253 Si ₃ N ₄	Room Temperature	540 MPa (78 ksi)	Fracture in attachment

Although the surface finish of the pin impacted the failure location and mechanism, the surface finish did not appear to have a significant effect on the failure load of the attachment specimens.

A comparison of the dovetail and pinned root attachment specimen testing at room temperature from each of the three suppliers is shown graphically in Figure 8. The room temperature failure stress of the dovetail root attachment specimens was considerably higher than the pinned root attachment specimens.

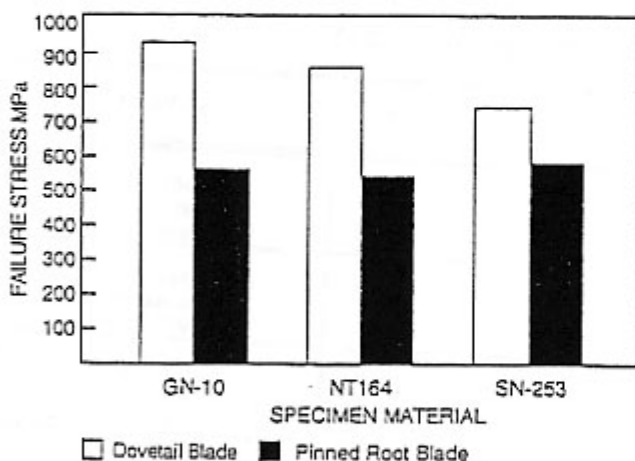


FIGURE 8. COMPARISON OF DOVETAIL AND PINNED ROOT ATTACHMENT SPECIMENS

The pinned root blade design has been modified to reduce design stress levels to ~255 MPa (37 ksi) from the original levels of 586 MPa (85 ksi). The modified pinned root attachment specimen is expected to provide a margin of safety by a factor of 2-3. Attachment specimens of the modified pinned root blade design have been fabricated in SN-253 (KICC) and will be tested under conditions similar to those for the dovetail design.

Cold spin testing will be conducted on simulated or dummy mass blades machined from attachment specimens and on actual blades. Spin test to rotational speeds that simulate engine CF blade loads on the simulated blades will be conducted at ambient conditions. Cold spin testing will also be performed on first and second generation

blades as a proof test. The blades will be tested at speeds that will be increased to 120% of the design stress. Blades that pass the proof test will be used in the gasifier rig test following Non Destructive Evaluation.

The SN 88 silicon nitride shows excellent dynamic fatigue behavior. It is believed that the composition of the sintering aid makes this material less susceptible to environmental degradation. Hexoloy SA is expected to have a very high slow crack growth resistance as well. However the strength of the silicon carbide is at least 138 MPa (20 ksi) lower than the SN 88 material in fast fracture. The very low values of m (Weibull modulus) for Hexoloy SA and NT 164 make them less attractive candidates for the nozzle. The presence of grinding media in the material may explain the extremely low value of m for Hexoloy SA. It should be noted that the number of NT 164 specimens so far tested is not sufficient to obtain an accurate determination of the Weibull modulus.

DYNAMIC FATIGUE TESTING FOR NOZZLES

As Fired Dynamic Fatigue Testing

The airfoil of the nozzle will be in the as-fired condition. Therefore dynamic fatigue testing of as-fired flexure bars at the nozzle airfoil peak temperature has been conducted on the candidate nozzle materials. Table 7 gives the results of this testing

Tensile Dynamic Fatigue Testing

Tensile dynamic fatigue testing of the four candidate nozzle materials was carried out at the University of Dayton Research Institute (UDRI). Twenty tensile specimens (10 at each crosshead speed) of each material were tested at 0.04 cm/s (0.95 in/min) and 0.000004 cm/s (0.000095 in/min). These tests were run on an Instron 1361 Universal Testing machine using the Instron "Super Grip" and Instron short furnace. The results of all the tests to date, are given in Table 8.

The failures were typically more surface dominated at the slower crosshead speed. NT 164 had all volume fracture origins at the faster crosshead speed, but of the ten at the slower crosshead speed eight failed at the surface. SN 253 had four volume fracture origins at the faster crosshead speed but all surface failures at the slower crosshead speed. Similarly SN 88 went from all volume related failures at the faster crosshead speed to six surface failures at the slower crosshead speed. This transition to more surface related failures suggests that

TABLE 7. DYNAMIC FATIGUE TESTING OF AS-FIRED FLEXURE BARS AT 1288°C (2350°F)

Matl/Prop	Number of Specimens Tested	Avg Strength Mpa (ksi)	Weibull Modulus, m	Standard Deviation Mpa (ksi)	Slow Crack Growth Exponent
NT 164 0.004 cm/s (0.095 in/min)	7	553 MPa (80.2)	4	117 (17)	50
NT 164 0.00004 cm/s (0.00095 in/min)	7	507 (73.5)	22	19 (2.82)	
SN 88 0.004 cm/s (0.095 in/min)	15	645 (93.6)	18	39 (5.7)	96
SN 88 0.00004 cm/s (0.00095 in/min)	15	586 (85)	31	24 (3.52)	
Hexoloy SA 0.004 cm/s	12	In Progress	In Progress	In progress	
Hexoloy SA 0.00004 cm/s (0.00095 in/min)	12	434 (63)	4	83 (12)	

TABLE 8. TENSILE DYNAMIC FATIGUE AT 1288°C (2350°F)

Matl/Prop	Number of Specimens Tested	Avg Strength Mpa (ksi)	Standard Deviation Mpa (ksi)	Slow Crack Growth Exponent (n)
NT 164 0.04 cm/s (0.95 in/min)	10	442 (64.1)	22 (3.2)	19
NT 164 0.000004 cm/s (0.000095 in/min)	10	276 (40)	39 (5.6)	
SN 253 0.04 cm/s (0.95 in/min)	10	590 (85.6)	27 (3.9)	21
SN 253 0.000004 cm/s (0.000095 in/min)	10	385 (55.9)	14 (2.0)	
SN 88 0.04 cm/s (0.95 in/min)	10	461 (66.8)	55 (8)	182
SN 88 0.000004 cm/s (0.000095 in/min)	10	438 (63.5)	17 (2.4)	
Hexoloy SA 0.04 cm/s (0.95 in/min)	10	453 (65.7)	56 (8.1)	65
Hexoloy SA 0.00004 cm/s (0.000095 in/min)	10	393 (57)	85 (12.3)	

the environment is inducing the surface cracks to grow at a faster rate, causing them to predominate over the volume defects. Analysis of defects on the surface at the two crosshead speeds did not give a value of n that differed significantly from data that had both surface and volume defects. SN88 tensile bars have a value of n equal to 182, that is higher than the value of $n = 96$ for flexure bars. Since n has an exponential relation with stress and stressing rate, a small variation of stress can result in a large variation of n . n above 80 essentially indicates no slow crack growth.

The NT 164 strength was considerably lower (103-138 MPa or 15-20 ksi) than data obtained for a similar NT 164 under the Ceramic Technology for Advanced Heat Engines (CTAHE) program in the same temperature range. On exposure to 1288°C (2350°F) the NT 164 specimens showed a spotted surface (Figure 9). Light element energy dispersive X-ray spectroscopy (EDS) using an Auger spectroscopy system revealed a relatively high concentration of sodium in this region (Figure 10). Figure 11 shows a volume fracture origin. EDS of this surface revealed an Fe inclusion, which seems to be a major cause of low strength fractures. Therefore the low strength failures appear to be caused both by migration of sodium from the encapsulant glass (used in the HIP process) to the dark surface areas causing premature failures and by the frequent presence of Fe inclusions.

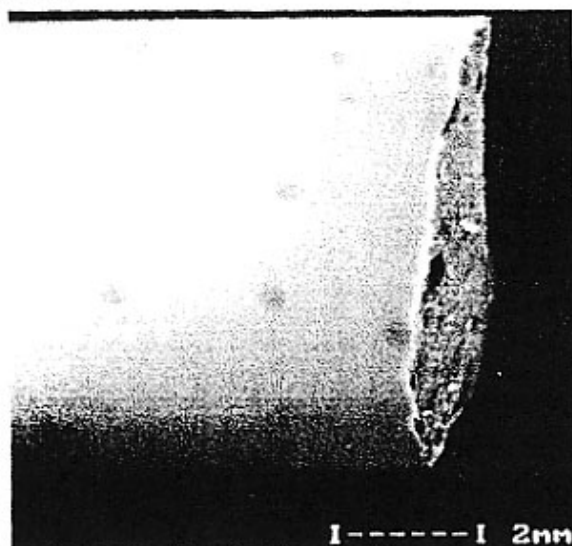


FIGURE 9. SPOTTED SURFACE ON TENSILE SPECIMEN SURFACE TESTED AT SLOWER CROSSHEAD SPEED (1288°C -2350°F)

The SN 253 material exhibited the highest Weibull modulus of any of the candidate materials. As a result the ratio of tensile strength to flexure strength of this material can be expected to be very high. The protrusions (Figure 4) on the surface appear to play a major role in the high Weibull modulus providing a consistent fracture initiation site. The degradation in average strength in going to the slower crosshead speed is almost 207 MPa (30 ksi) and all the failures were surface related.

SN 88 has a lower fast fracture strength as compared to SN 253 but it retains almost all of its strength at the slower crosshead speed (exhibiting less strength reduction than the silicon carbide). The extent

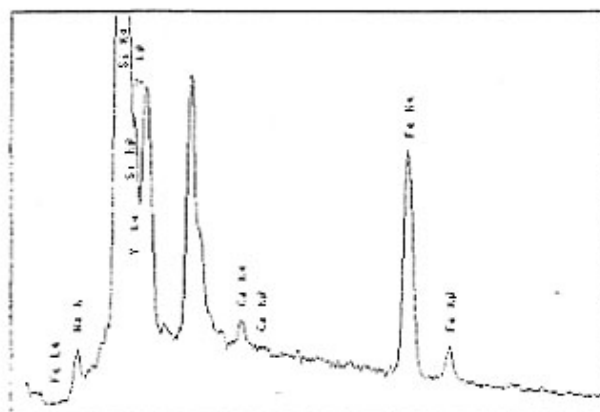


FIGURE 10. EDS OF SPOTS SHOWING HIGH CONCENTRATION OF SODIUM



FIGURE 11. TYPICAL VOLUME INCLUSION INITIATED SURFACE. INCLUSION USUALLY HAS HIGH IRON CONCENTRATION

of strain before failure is unusually high as compared to the other silicon nitrides. The Hexaloy SA shows minimal degradation at the slower crosshead speed. The strength of the material however is lower than the silicon nitrides tested with the exception of NT 164. Static fatigue and stress relaxation tests have already commenced at UDRI and at ORNI (Ferber et al., 1994)

SUMMARY

Evaluation of various silicon nitrides and one grade of silicon carbide are being performed in support of the Ceramic Stationary Gas Turbine project. Results to date have helped fill gaps in literature that are considered crucial for design and life prediction in this application.

Dynamic fatigue tests were conducted on candidate materials at room temperature, 760°C and 1093°C. At room temperature the slow

crack growth exponents(n) of the three candidate blade materials GN-10, NT 164 and SN 253 were determined to be 24, 26 and 100 respectively. At 760° C the n values were 28 for GN-10, 38 for NT 164 and 112 for SN 253. NT 164 is the only material tested at 1093° C and the n value is 44. More variability was encountered in testing specimens with as-fired surfaces with fractures originating at pores and iron inclusions.

Blade attachment tests showed 2-4 times failure stress margin for the dovetail blade design. Tests on the pinned root configuration led to a redesign of the geometry to provide higher margins.

Tensile dynamic fatigue tests on candidate nozzle materials at 1288° C gave n values of 182, 65, 21 and 19 for SN 88, Hexoloy SA, SN 253 and NT 164 respectively.

ACKNOWLEDGMENT

The work presented in this paper was performed on DOE contract DE-AC02-92CE40960. The authors would like to thank W.D. Parks and S. Waslo of DOE as well as M. Van Roode Solar CSGT Program Manager for their guidance and encouragement. Matt Ferber at ORNL has been extremely supportive of this effort and provided both laboratory help and technical advice. Assistance received from A. Livingstone and A. Burke of Solar Turbines is also gratefully acknowledged.

REFERENCES

Hecht N.L. et al., 1990, "The Evaluation of Environmental Effects in Toughened Ceramics for Advanced Heat Engines Investigation of Selected Si₃N₄ and SiC Ceramics,"ORNL/SUB/84-00221, Oak Ridge National Laboratory .

Carruthers D. et al., 1994, "Dynamic Fatigue Data, SN 253", Kyocera Memo 024.

Ferber M.K. et al., 1994, "Long Term Testing of Ceramics For Industrial Gas Turbines", Advanced Turbine Systems Material/Manufacturing Bimonthly Report, Oak Ridge National Laboratory.

Weiderhorn, S. M., et al., 1974, " Subcritical Crack Growth", "Fracture Mechanics of Ceramics, Pgs 613-646, Vol.2, R. Bradt et al., Plenum Press, N.Y.